Environ. Eng. Res. 2018; 23(3): 250-257
https://doi.org/10.4491/eer.2017.096

pISSN 1226-1025
eISSN 2005-968X

New composites based on low-density polyethylene and rice husk: Elemental and thermal characteristics

Muhammad Anshar[1], Dahlang Tahir[2†], Makhrani[2], Farid Nasir Ani[3], Ab Saman Kader[4]

[1]*Department of Mechanical Engineering, State Polytechnic of Ujung Pandang, Makassar 90245, Indonesia*
[2]*Department of Physics, Hasanuddin University, Makassar 90245, Indonesia*
[3]*Department of Thermodynamics and Fluid Mechanics, Universiti Teknologi Malaysia, Skudai-Johor 81310, Malaysia*
[4]*Marine Technology Centre, Universiti Teknolgi Malaysia, Skudai-Johor 81310, Malaysia*

ABSTRACT

We developed new composites by combining the solid waste from Low-Density Polyethylene in the form of plastic bag (PB) and biomass from rice husk (RH),in the form of $(RH)_x(PB)_{1-x}$ (x = (1, 0.9, 0.7, 0.5)), as alternative fuels for electrical energy sources, and for providing the best solution to reduce environmental pollution. Elemental compositions were obtained by using proximate analysis, ultimate analysis, and X-ray fluorescence spectroscopy, and the thermal characteristics were obtained from thermogravimetric analysis. The compositions of carbon and hydrogen from the ultimate analysis show significant increases of 20-30% with increasing PB in the composite. The activation energy for RH is 101.22 kJ/mol; for x = 0.9 and 0.7, this increases by 4 and 6 magnitude, respectively, and for x = 0.5, shows remarkable increase to 165.30 kJ/mol. The range of temperature of about 480-660°C is required for combustion of the composites $(RH)_x(PB)_{1-x}$ (x = (1, 0.9, 0.7, 0.5)) to perform the complete combustion process and produce high energy. In addition, the calorific value was determined by using bomb calorimetry, and shows value for RH of 13.44 MJ/kg, which increases about 30-40% with increasing PB content, indicating that PB has a strong effect of increasing the energy realized to generate electricity.

Keywords: Elemental composition, Low-density polyethylene, Plastic bags, Rice husk, Thermal characteristics

1. Introduction

Clean and efficient utilization of biomass as a source of alternative energy is of major concern, and is essential for generating electricity, especially in developing countries. Indonesia as a developing country is still lacking in electrical energy supply, with electrification of around 76.56% [1]. About 23.5% of rural communities have not yet used electrical energy, due to the inability of power plants to meet the increasing power needs of the society and industry every year. More than half of the electricity suppliers in Indonesia generate their electricity from coal [2]. Coal production in Indonesia is quite large, at around 2.751×10^8 tons in 2010 [3]. However, continuous mining and combustion of coal as fuel damages the natural environment. On the other hand, Indonesia has abundant potential biomass resources that are environmentally friendly. The potential of rice husk (RH) in 2012 was around 1.381×10^7 tons, equivalent to the electrical energy potential of around 53.702 GWh, the third largest in the world after China and India [4, 5]. Nonetheless, this potential has not been exploited, and few have reported it as a source of energy [6]; it has only been used as a catalyst [7, 8], or wasted, causing environmental pollution. In Indonesia, large amounts of biomass fuels are consumed for cooking, and some biomass of low density, such as RH, is used for heating. The burning of biomass fuel is one of the most important sources of emission of CO and volatile organic matter, which not only cause severe indoor air pollution, but also contribute to regional, global, and climate forcing. Replacing traditional fuel methods with cleaner techniques are challenges in several countries, including Indonesia. Several alternative options that are expected to result in lower emission pollution than traditional burning include pellets and catalyst. However, some studies reported the preparation of RH as pellets or catalyst to be time-consuming and energy intensive, due to low-density biomass, generally performed under high temperature (400-800°C), and long reaction time (up to 15 h) [9-11].

Received July 26, 2017 **Accepted** February 6, 2018

† Corresponding author
Email: dtahir@fmipa.unhas.ac.id
Tel: +62-411-587634 Fax: +62-411-587634
ORCID: 0000-0002-8241-3604

RH is also a widely accepted alternative energy source, due to its high carbon and oxygen composition, which is fundamental for searching sources of energy [12, 13]. Direct combustion in a grate bed combustor can minimize harmful exhaust gasses by using an exhaust emission control device, which is a technique that uses RH as fuel for power plants to generate electricity in Thailand [12], and India [13]. Generating electricity from biomass provides significant benefits to the environment, since it produces clean energy [14].

In addition to the electrical energy shortage, Indonesia also has problems in handling municipal solid waste (MSW), particularly low-density polyethylene (LDPE) type plastic bags (PB). The average household solid waste generated in Jakarta and another big city in Indonesia is 2,416.2 kg per household per year, with PB (14%) being the second largest, and increases every year by about 2-5% [15, 16]. PB at landfills may take tens to hundreds of years to be completely decomposed, and subsequently, those particles could contaminate the soil and water of the surrounding area [17]. In fact, PB has a calorific value (CV) of about 41.5 MJ/kg [18]. PB combustion in the grate bed combustor can be controlled by using an exhaust emission control device to minimize harmful exhaust gasses [19-21], and PB isalso used as fuel for power plants to generate electric power of about 8.9 MW in Malaysia [21-25].

Based on the fuel needed for generating electricity, and the potentials of solid waste and biomass, in this study, we developed new composites by combinations of solid waste and biomass in the form of $(RH)_x(PB)_{1-x}$ (x = (1, 0.9, 0.7, 0.5)) as alternative fuels for electrical energy sources, and on the other hand, giving the best alternative solution to reduce environmental pollution. We focus in this study on discussing the effect of PB in terms of elemental composition, by using proximate analysis, ultimate analysis, and X-ray fluorescence (XRF) and thermal characteristics, including activation energy, by using thermogravimetric analysis.

2. Materials and Methods

2.1. Materials Preparation

The samples in this study are composites $(RH)_x(PB)_{1-x}$ (x = (1, 0.9, 0.7, 0.5)) from RH and PB as alternative energy sources. We chose PB type LDPE identified by the logo triangle figure in the middle of the LDPE sign, which is usually used for shower curtains, packaging, films, and clamshell. After being sun-dried, RH and PB were cut and ground to reduce size using a mill. Raw materials were sieved to obtain uniformity of size of between 0.125 and 0.3 mm (for details, see [4, 22]). The physical mixing of samples was performed by weighting each raw sample to form composites $(RH)_x(PB)_{1-x}$ (x = (1, 0.9, 0.7, 0.5)) by using a digital balance. The mass of composite samples was fixed at about 10 g. The samples were mixed withstirring for 15 min to obtain uniform and homogeneous composites. The samples were heated at 105℃ temperature for one hour and seven hours for PB and RH, respectively (for details, see [23]), and for composites were the weighted average time of heating of RH and PB.

2.2. Proximate Analysis, Ultimate Analysis, and Calorific Value

The chemical compositions of composites $(RH)_x(PB)_{1-x}$ (x = (1, 0.9, 0.7, 0.5)) were determined from the proximate analysis, ultimate analysis, and XRF spectroscopy. The proximate and ultimate analyses were conducted based on the Standard Methods ASTM D 3172 - D 3174, ASTM D 4239, ASTM D 5373, and ISO 565. Meanwhile, the CV was carried out by using bomb calorimeter according to the Standard Methods ASTM D.5865 (for details, see [26, 27]).

2.3. Oxidative and Kinetic Study

The oxidative study of the $(RH)_x(PB)_{1-x}$ (x = (1, 0.9, 0.7, 0.5)) was conducted to determine the characteristics of the kinetic parameter based on the some previous studies [28-32], by using thermal gravimetric analysis (TGA) and differential thermal gravimetric (DTG). The oxidative reaction was carried out from temperature 30 to 800℃ for about 82 min, at a heating rate of about 10℃/min, and flow rate of air of about 50 mL/min. The Mettler test was performed on the $(RH)_x(PB)_{1-x}$ (x = (1, 0.9, 0.7, 0.5)) samples, with a mass test of about 5.5-5.8 mg. The characteristics of $(RH)_x(PB)_{1-x}$ (x = (1, 0.9, 0.7, 0.5)) from TGA and DTG were analyzed by using Sma4Winsoftware. A two-stage reaction kinetic scheme has been proposed for the thermal degradation (TD) of composites under an oxidative atmosphere [31], representing the DTG curves:

First stage: A (solid) $\longrightarrow$ B (char) + C1 (gas) (1)

Second stage: B (char) $\longrightarrow$ C2 (gas) + D (ash) (2)

The kinetic parameters were calculated from the linear regression curve with the correlation factors (above 0.90), based on the Arrhenius law. The activation energy (Ea) that occurs at every TD process [33-35] was determined by using the following equations:

$$k = Ae^{(-Ea/RT)} \tag{3}$$

where, k is the reaction rate, Ea is the activation energy for the reaction (J/mol), A is the pre-exponential factor (1/min), R is the universal gas constant (8.314 J/K mol), and T is the absolute temperature (K). The equation can be written in logarithmic form:

$$\ln k = \ln A - \left(\frac{Ea}{RT}\right)\ln e \tag{4}$$

where, ln e = 1

$$\ln k = -\frac{Ea}{R} \times \frac{1}{T} + \ln A \tag{5}$$

Based on previous studies [33, 36, 37], the Eq. (5) was obtained:

$$\ln k = -\ln\left[\frac{\ln(1-\alpha)}{T^2}\right] \text{ and } \ln A = \ln\frac{AR}{\beta E}$$

Thus, Eq. (5) can be written as:

$$-\ln\left[\frac{\ln(1-\alpha)}{T^2}\right]=\frac{Ea}{R}\times\frac{1}{T}+\ln\frac{AR}{\beta E} \quad (6)$$

where, β is the heating rate (K/min). The mass loss fraction α (mg) for every stage of the thermal degradation is defined as:

$$\alpha=\frac{Mi-Ma}{Mi-Mf} \quad (7)$$

where, *Mi* is the initial mass of the sample at the beginning reaction (mg), *Ma* is the actual mass of the sample (mg), and *Mf* is the final mass, or the mass after oxidation of the sample (mg). The *Ea* may then be extracted from a plot of ln *k* vs. *1/T*, which should be linear. Eq. (5) can be analogous to the equation of a straight line, which is often symbolized by the linear regression equation$y = mx + b$. Thus, the $-\ln\left[\frac{\ln(1-\alpha)}{T^2}\right]$ is they-axis, $\frac{1}{T}$ is the x-axis, and $b=\ln\frac{AR}{\beta E}$ is the intercept of the line with the y-axis, with $m=\frac{Ea}{R}$ as slope. The *Ea* is obtained for every step of degradation (mass loss) [33, 37, 38].

3. Results and Discussion

Table 1 shows the results of the proximate and ultimate analyses of $(RH)_x(PB)_{1-x}$ (x = (1, 0.9, 0.7, 0.5)). For RH, it shows good agreement with previous results [38] for elemental composition (fixed carbon (FC), volatile matter (VM), ash (A) content, carbon (C), hydrogen (H), and oxygen (O)), with differences <10%. We also compared the results with several reported in previous studies [39-42] for the value of moisture content (MC), VM, FC, nitrogen (N), sulphur (S), O, H, and A, where the values were similar. This shows that the parameters of the test results and methodology used in this study show good accuracy, with acceptable values. The most important elements for energy application, which must be of high content, are C, FC, H, and MC, but other elements should be low. PB shows high C and H, and low A, MC, N, O, and S; while RH shows high FC and MC. By mixture of RH and PB to form composites, a good characteristic element can be obtained for the release of energy. Table 1 shows that composites $(RH)_x(PB)_{1-x}$ (x = (0.9, 0.7, 0.5)) reveal homogeneous samples; all elemental composition is increased gradually with increasing PB content for an element with higher content in PB, and vice versa.

For C, H, and O, we have compared with the results of predictive equation by using data from proximate analysis as input

Table 1. Elemental Composition by Using Proximate and Ultimate Analysis, and Calorific Value from Bomb Calorimeter in Oxygen Environment for Composites $(RH)_x(PB)_{1-x}$ (x=1, 0.9, 0.7, 0.5). We Have Included Elemental Composition for RH from [31], Calculation Based on Predictive Equation for Carbon, Hydrogen, and Oxygen from [35, 36], and for Calorific Value from [37] for Comparison

Parameter	Unit	RH (Present Study)	RH [31]	10%PB	30%PB	50%PB	PB
Proximate Analysis							
Fixed carbon (FC)	(%)	14.81	16.95	13.62	10.89	8.00	0.72
Volatile matter (VM)	(%)	55.62	61.81	58.65	65.21	72.39	89.04
Moisture content (M)	(%)	10.46		9.68	7.53	5.26	0.22
Ash (A)	(%)	19.11	21.24	18.05	16.37	14.35	10.02
Ultimate Analysis							
Carbon	(%)	37.48	38.50	40.21	47.00	53.60	67.49
Predictive [35]	(%)	32.68		33.09	33.97	35.01	36.76
Predictive [36]	(%)	41.91		42.13	42.49	42.98	43.57
Hydrogen	(%)	5.08	5.20	5.82	7.10	8.61	10.25
Predictive [35]	(%)	9.92		9.69	8.91	8.11	6.38
Predictive [36]	(%)	4.09		4.28	4.64	4.98	0.17
Oxygen	(%)	37.81	34.61	35.45	29.13	23.08	11.92
Predictive [35]	(%)	51.92		51.73	50.29	48.91	46.19
Predictive [36]	(%)	24.92		26.39	29.56	33.04	41.08
Nitrogen	(%)	0.43		0.38	0.31	0.28	0.26
Sulfur	(%)	0.09		0.09	0.09	0.08	0.06
Ash	(%)	19.11		18.05	16.37	14.35	10.02
Calorific and Bulk							
Calorific value	(MJ/kg)	13.44		17.85	23.97	28.93	41.21
Predictive [37]	(MJ/kg)	21.81		22.52	24.01	25.68	29.31
Bulk density	(kg/m^3)	265		228,5	198,8	167.6	112

parameter, proposed by [43] in the form: C = -35.9972 + 0.7698*VM* + 1.3269*FC* + 0.3250*A*, H = 55.3678 - 0.4830*VM* - 0.5319*FC* - 0.5600*A*, O = 223.6805 - 1.7226*VM* - 2.2296*FC* - 2.2463*A*, and those proposed by [42] in the form: C = 0.47*VM* + 0.963*FC* + 0.067*A*, H = 0.074*VM* + 0.012*FC* - 0.052(*VM*/*FC*), O = 0.569*VM* + 0.010*FC* - 0.069*A*. The predictive proposed by Nhuchhen [43] shows reasonable agreement for RH with differences of about 10%, while the predictive proposed by Thomas Klasson [44] shows good agreement for 10%PB in composites. The C content from the ultimate analysis in this study shows an increase with increasing PB content in composites that is consistent with the result from predictive equation from [43], with differences of about 15% lower than the ultimate analysis data. The predictive equation from [44] shows that C content is higher for RH, and increases by about 0.5% with increasing PB content in composites. For H, good agreement is shown between the predictive equation from [44] only for RH, and from [43] only for 30%PB and 50%PB, compared with the ultimate analysis data. For O, the content shows a big difference of about 30-40% between the ultimate analysis data with predictive from [43], and good agreement only for 30% PB with the predictive from [44]. These results indicated that the existing predictive equations from [43] and [44] show good accuracy in results compared with the ultimate analysis data only for several compositions in composites RH and PB.

Table 1 shows that we compared the CV determined by bomb calorimetry in this study with the predictive model developed by Majumder *et al.* [45] in the form CV (MJ/kg) = -0.03*A* - 0.11*M* + 0.33*VM* + 0.35*FC*. RH shows CV of about 13.44 MJ/kg, which is very good agreement with [40] of about 13.30 MJ/kg, and [41] of about 13.50 MJ/kg; and PB shows CV of about 41.21 MJ/kg in this study, which is also comparable with the previous studies [46-48]. For composites, the CV was increased by about 30% with increasing PB content in composites. The differences between predictive equations with the result in this study for 30 and 50% PB in composites are about 10%, but become high for pure RH and PB. This indicated that the predictive CV from [45] is valid for high PB content in composites, and shows good agreement with ethanol (30 MJ/kg) and methanol (23 MJ/kg) as acceptable fuels [49].

For composites $(RH)_x(PB)_{1-x}$ (x = (0.9, 0.7, 0.5)), the CV increased with increasing amount of PB to RH from 17.85 MJ/kg for x = 0.9, 23.97 MJ/kg for x = 0.7, to 28.93 MJ/kg for x = 0.5. Moreover, increasing the CV showed a positive correlation with C, H, and VM of the fuel. In contrast, the addition of PB lowered the percentage of O, S, N, FC, MC, and A. The physical properties of the fuel depend on the content of CV, MC, and AC that influence the energy production. The amount of MC in the fuel affected the CV and A of the combustion products [35]. One would expect the fuel mixture to have a maximum CV and minimum A. The energy and power that can be generated depend on the CV content in the composites for fuel.

The addition of PB to RH can improve the quality of fuel, such as increasing CV, C, H, and VM, and decreasing FC, MC, S, N, O, and A. The increasing content of C and H means a greater contribution to the energy released [35]. However, the percentage of O decrease in the fuel means increasing the content of C and H, as well as increasing CV of the fuel, but O is required in the process of fuel combustion. The high CV can increase energy production; thus, composites in this study become attractive as an energy source. Small amounts of N will reduce NO_x emissions in the air, while small amounts of S can reduce pollution and corrosion. High amounts of VM and A and low MC are important characteristics required in the process of energy production. The high amount of A is affected by the reduction of energy production, and an increase of handling cost for the disposal process [50]. High MC will aggravate the chemical properties of the fuel, hence complicating the process of energy production. The increasing amount of PB in composites resulting in decrease in the amount of N and S indicated the formation of NO_x and SO_x is decreased; these are both hazardous gasses, and very harmful to the environment [51-53]. Thus, the addition of PB into RH to form composites will increase energy production, and also decrease the amount of MC, A, NO_x, and SO_x.

Table 2 shows the elemental composition by using XRF spectroscopy after heating the composites at the temperature of 105℃ for several hours. The main elements for ash from RH are Si and K of about 73.61 and 14.31%, respectively, which are similar to those reported in Refs. [26, 27], and those for ash from PB are Ca and Ti of about 75.61 and 12.93%, respectively, which are similar values to those reported in [54]. The composites show Si and K as the main elements of ash from RH decrease

Table 2. Elemental Composition by Using X-ray Fluorescence (XRF) for Composites $(RH)_x(PB)_{1-x}$ (x = 1, 0.9, 0.7, 0.5) after 105℃ for Several Hours

Element	RH	10%PB	30%PB	50%PB	PB
Si	73.61	63.35	34.61	31.99	2.98
K	14.31	6.81	4.00	2.40	-
Ca	3.51	18.25	52.89	57.75	75.61
Cl	2.78	2.55	1.64	-	-
Px	2.33	3.84	0.73	0.57	-
Fe	2.06	0.97	-	-	-
Ti	-	1.26	5.57	6.16	12.93
Mg	-	-	-	-	7.05
Pb, Zn, Cr, Mn, Nb, Mo, In	1.4	2.97	0.56	1.13	1.43

with increasing the amount of PB, and similarly, the elements of ash from PB areincreased with increasing the amount of RH.

TGA and DTG curves show that there is a difference between the oxidation process of $(RH)_1(PB)_{1-x}$ (x = (1, 0.9, 0.7, 0.5)), as shown in Fig. 1. The TGA and DTG curves of $(RH)_x(PB)_{1-x}$ (x = (1, 0.9, 0.7, 0.5)) show the dehydration process (DP) with degradation temperature (DT) from 40 to 100℃ and mass loss (ML) from 2.3 to 5.2%, as moisture evaporation indicated the dehydration processes. The TD of composites is of two stages for $x \geq 0.7$, and of three stages for x = 0.5. TD in the first zone (TDZ1) is in the range of temperature 240-360℃ with ML in the range 40.4-43.7%, while TDZ2 is in the range of temperature of 370-490℃, with ML in the range 25.4-32.6%. Furthermore, TDZ3 is in the range of temperature 600-670℃, with ML of about 2.8%. The total ML during the degradation of $(RH)_1(PB)_{1-x}$ (x = (1, 0.9, 0.7, 0.5)) is in the range 71.6-79%, and generated A approximately in the range 21-28.4%. This shows that the addition of PB to RH influences the thermal characteristics of composites by enlarging the energy production and reducing the A residues. Table 3 shows the parameters of kinetic study for the oxidative environment of $(RH)_1(PB)_{1-x}$ (x = (1, 0.9, 0.7, 0.5)).

Fig. 2 shows the *Ea* that occurred in the TDZ1 of the $(RH)_1(PB)_{1-x}$ (x = (1, 0.9, 0.7, 0.5)). The activation energy for the TDZ1 of RH of 56.49 kJ/mol was obtained on the basis of the linear regression: $y_1 = 6{,}794x + 1.902$, with $R^2 = 0.915$ for DT in the

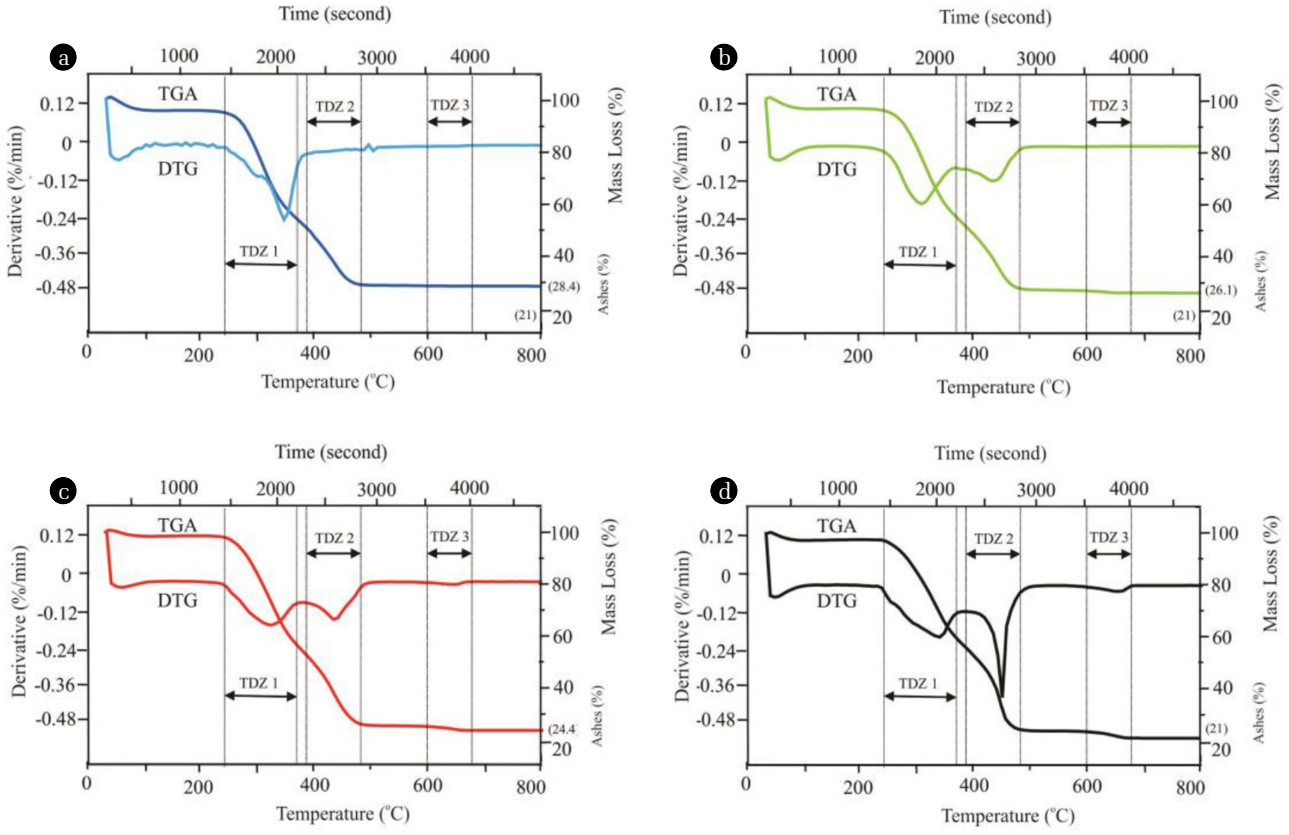

Fig. 1. TGA and DTG spectra for the temperature range 30-800°C with a heating rate of 10°C/min and flow rate of air of about 50 mL/min fromcomposites $(RH)_x(PB)_{1-x}$, for (a) x = 1, (b) x = 0.9 , (c) x = 0.7, and (d) x = 0.5.

Table 3. Parameters of the Kinetic Study for the Oxidative Environment of Composites $(RH)_x(PB)_{1-x}$ (x = 1, 0.9, 0.7, 0.5) for Thermal Degradation Zone (TDZ1, TDZ2, TDZ3) Based on Fig. 1

Materials	MS (mg)	DP		TDZ1		TDZ2		TDZ3		EaT (kJ/mol)	Ash (%)
		ML (%)	T (°C)	ML (%)	T (°C)	ML (%)	T (°C)	ML (%)	T (°C)		
RH	5.8	5.2	50-100	41	240-360	25.4	370-480	-	-	101.22	28.4
10%PB	5.5	4.4	50-100	43.7	240-360	25.8	370-490	-	-	104.03	26.1
30%PB	5.6	2.3	50-100	42.4	250-380	27.9	390-490	-	-	110.95	24.4
50%PB	5.5	3.2	50-100	40.4	250-380	32.6	390-460	2.8	600-670	165.30	21

range 240-360℃ (Fig. 2(a)). The Ea_1 of 10%PB of 55.55kJ/mol was based on the equation: $y_1 = 6{,}681x + 2.340$ with $R^2 = 0.978$ for DT in the range 240-380℃ (Fig. 2(b)). For 30%PB, the Ea_1 is 64.63kJ/mol, based on the equation: $y_1 = 7{,}774x + 0.721$ with $R^2 = 0.959$ for DT in the range 250-380℃ (Fig. 2(c)). Furthermore, the Ea_1 of 50%PB is 54.42kJ/mol based on the equation: $y_1 = 6{,}546x + 3.005$ with $R^2 = 0.979$ for DT in the range 250-380℃ (Fig. 2(d)). By the same method, Table 4 shows the equation and *Ea* for the TD process in the second (TDZ2) and the third zones (TDZ3) obtained by linear regression.

Table 4 clearly shows that the amount of PB in composites is important in increasing the *Ea* value. The higher contents of PB in composites are the higher values of *Ea*. The oxidative process of the TD processes for RH was perfect after reaching a temperature of about 480℃, and increased to 490℃ for 10 and 30%PB. For 50%PB, the TD process was perfect after reaching

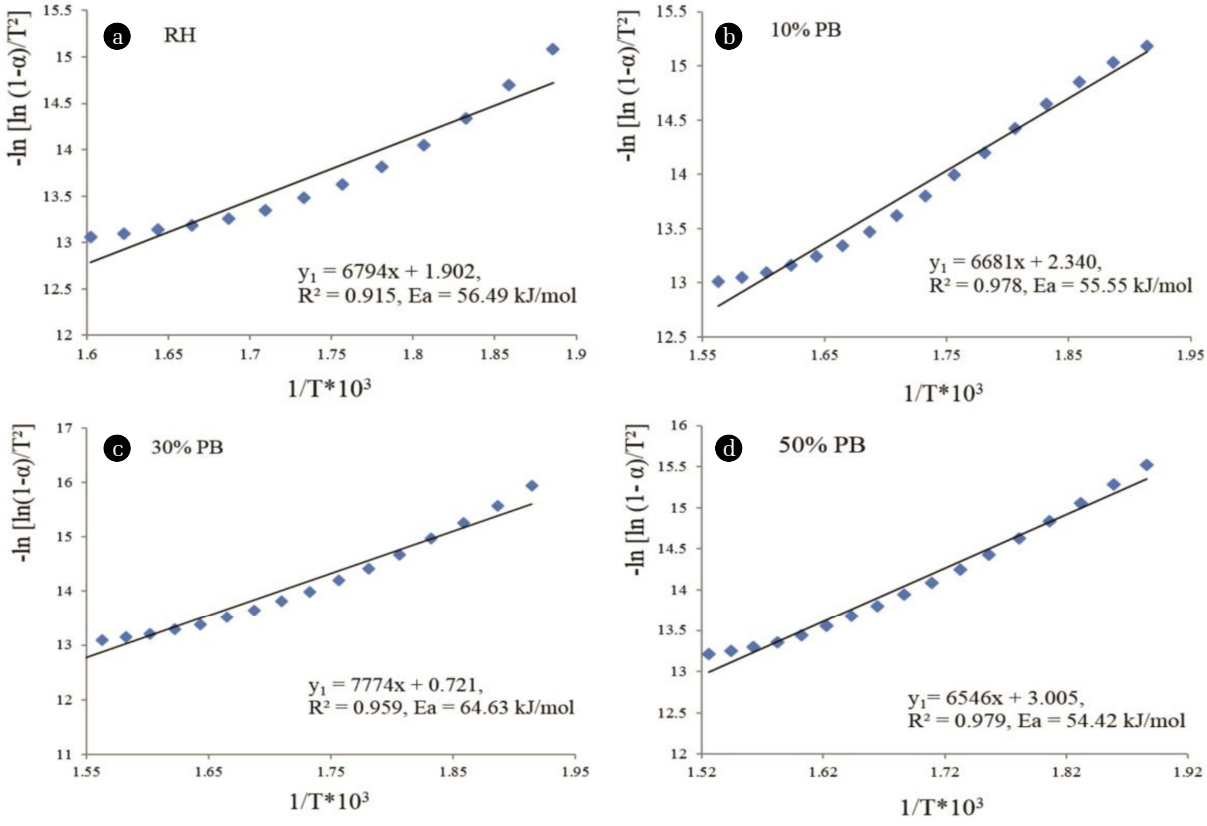

Fig. 2. The first degradation (TDZ1) stage of the oxidative process to determine activation energy (E_a) and R^2 values from the linear regression of -ln [ln (1- α)/T^2] vs. 1/T for composites $(RH)_x(PB)_{1-x}$, for (a) x = 1, (b) x = 0.9 , (c) x = 0.7, and (d) x = 0.5.

Table 4. Thermal Degradation Process for Zone 1, 2, 3 to Determine Activation Energy (Ea) by Using Linear Regression (as Shown in Fig. 2 for TDZ1) of Arrhenius Law from Analysis Data of TGA and DTG in Fig. 1

Samples	DT (°C)	Linear regression of Arrhenius law	(R^2)	Ea (kJ/mol)			
				Ea1	Ea2	Ea3	Total
RH	240-360	$y_1 = 6{,}794x + 1.902$	0.915	56.49	-	-	-
	370-480	$y_2 = 5{,}380x + 4.792$	0.916	-	44.73	-	101.22
10%PB	240-380	$y_1 = 6{,}681x + 2.340$	0.978	55.55	-	-	-
	390-490	$y_2 = 5{,}831x + 4.216$	0.961	-	48.48	-	104.03
30%PB	250-380	$y_1 = 7{,}774x + 0.721$	0.959	64.63	-	-	-
	390-490	$y_2 = 5{,}571x + 4.627$	0.971	-	46.32	-	110.95
50%PB	250-380	$y_1 = 6{,}546x + 3.005$	0.979	54.42	-	-	-
	390-460	$y_2 = 6{,}444x + 3.637$	0.915	-	53.58	-	-
	600-660	$y_3 = 6{,}892x + 4.695$	0.924	-	-	57.30	165.3

a temperature of about 660℃, and from temperature in the range 660-800℃, there was no TD or ML. This shows that the composites $(RH)_1(PB)_{1-x}$ (x = (1, 0.9, 0.7, 0.5)) combustion as fuel requires a temperature range of about 480-660℃ to perform the complete combustion process to produce high energy.

4. Conclusions

New composites $(RH)_x(PB)_{1-x}$ (x = 1, 0.9, 0.7, 0.5) have been obtained, and show gradually increased elemental composition with increasing PB content for an element with higher content in PB, and decrease with increasing PB for lower content in PB, indicating a homogeneous composite sample. The CV determined by bomb calorimetry shows about 13.44 MJ/kg for RH, and about 41.21 MJ/kg for PB, for composites, which was increased by about 30% with increasing PB content in composites, indicating PB has a strong effect on the composites.

The temperature range that produced the highest energy and performed complete combustion process of the composites $(RH)_x(PB)_{1-x}$ (x = (1, 0.9, 0.7, 0.5)) is 480-660℃. The activation energy for RH is 101.22 kJ/mol, which increases by (4 and 6) magnitude for x = (0.9 and 0.7), respectively, and increases remarkably to 165.30 kJ/mol for x = 0.5. The thermal characteristics, calorific value, and elemental analysis show the activation energy, calorific content, carbon, and hydrogen content, respectively, were strongly affected by the PB content, which contributed to increasing the realized energy.

Acknowledgments

The authors would like to thank the Kementerian Ristek-Dikti, Republic of Indonesia, for financial support through the Post-Doctoral Program, 2017.

References

1. Qodri FE, Widodo WP, Mahmud S, Akhmad H. An assessment of Indonesia's energy security index and comparison with seventy countries. *Energy* 2016;111:364-376.
2. Tobias SS, Nicola UB, Ratri SW. Attracting private investments into rural electrification – A case study on renewable energy based village grids in Indonesia. *Energy Sust. Dev.* 2013;17:581-595.
3. Friederich MC, Moore TA, Flores RM. A regional review and new insights into SE Asian Cenozoic coal-bearing sediments: Why does Indonesia have such extensive coal deposits? *Int. J. Coal Geol.* 2016;166:2-35.
4. Anshar M, Kader AS, Ani FN. The utilization potential of rice husk as an alternative energy source for power plants in Indonesia. *Adv. Mater. Res.* 2014;845:494-498.
5. Nicola UB, Ratri SW, Tobias SS. Rural electrification through village grids – Assessing the cost competitiveness of isolated renewable energy technologies in Indonesia. *Renew. Sust. Energy Rev.* 2013;22:482-496.
6. Zhao B, Li BX. The effect of sodium chloride on the pyrolysis of rice husk. *Appl. Energ.* 2016;178:346-352.
7. Al-Amsyar SM, Adam F, Eng-Poh N. Aluminium oxide-silica/carbon composites from rice husk as a bi-functional heterogeneous catalyst for the one-pot sequential reaction in the conversion of glucose. *Surface. Interface.* 2017;9:1-8.
8. Touhami D, Zhu Z, Balan WS, Janaun J, Haywood S, Zein SH. Characterization of rice husk-based catalyst prepared via conventional and microwave carbonization. *J. Environ. Chem. Eng.* 2017;5:2388-2394.
9. Budarin VL, Zhao Y, Gronnow MJ, et al. Microwave-mediated pyrolysis of macro-algae. *Green Chem.* 2011;13:2330.
10. Chen WH, Ye SC, Sheen HK. Hydrolysis characteristics of sugarcane bagasse pretreated by dilute acid solution in a microwave irradiation environment. *Appl. Energ.* 2012;93: 237-244.
11. Zhu Z, Macquarrie DJ, Simister R, Gomez LD, Mason SJM. Microwave assisted chemical pretreatment of Miscanthus under different temperature regimes. *Sust. Chem. Process.* 2015;3:1-13.
12. Madhiyanon T, Sathitruangsak P, Soponronnarit S. Co-combustion of rice husk with coal in a cyclonic fluidized-bed combustor (ψ-FBC). *Fuel* 2009;88:132-138.
13. Kapur T, Kandpal TC, Garg HP. Electricity generation from rice husk in Indian rice mills: Potential and financial viability. *Biomass Bioenerg.* 1996;10:393-403.
14. Liu J, Wang S, Wei Q, Yan S. Present situation, problems and solutions of China's biomass power generation industry. *Energ. Policy* 2014;70:144-151.
15. Aretha A, Tetsuo T, Gert S. Inorganic and hazardous solid waste management: Current status and challenges for Indonesia. *Procedia Environ. Sci.* 2013;17:640-647.
16. Yeny D, Yulinah T, Sony S. Community participation in household solid waste reduction in Surabaya, Indonesia. *Resour. Conserv. Recy.* 2015;102:153-152.
17. Lino FAM, Ismail KAR. Analysis of the potential of municipal solid waste in Brazil. *Environ. Dev.* 2012;4:105-113.
18. Zhou C, Fang W, Xu W, Cao A, Wang R. Characteristics and the recovery potential of plastic wastes obtained from landfill mining. *J. Clean. Prod.* 2014;80:80-86.
19. Wong SL, Ngadi N, Abdullah TAT, Inuwa IM. Current state and future prospects of plastic waste as source of fuel: A review. *Renew. Sust. Energ. Rev.* 2015;50:1167-1180.
20. Tabasová A, Kropáč J, Kermes V, Nemet A, Stehlík P. Waste-to-energy technologies: Impact on environment. *Energy* 2012;44:146-155.
21. Othman MR, Martunus, Zakaria R, Fernando WJN. Strategic planning on carbon capture from coal-fired plants in Malaysia and Indonesia: A review. *Energ. Policy* 2009;37:1718-1735.
22. Chen D, Zheng Y, Zhu X. In-depth investigation on the pyrolysis kinetics of raw biomass. Part I. Kinetic analysis for the drying and devolatilization stages. *Bioresour. Technol.* 2013;131:40-46.
23. Xie Z, Ma X. The thermal behavior of the co-combustion between paper sludge and rice straw. *Bioresour. Technol.* 2013;146:611-618.

24. Hiloidhari M, Baruah DC. Crop residue biomass for decentralized electrical power generation in rural areas (part 1): Investigation of spatial availability. *Renew. Sust. Energ. Rev.* 2011;15:1885-1892.
25. Hiloidhari M, Baruah DC. Rice straw residue biomass potential for decentralized electricity generation: A GIS-based study in Lakhimpur district of Assam, India. *Energ. Sust. Dev.* 2011;15:214-222.
26. Maiti S, Dey S, Purakayastha S, Ghosh B. Physical and thermochemical characterization of rice husk char as a potential biomass energy source. *Bioresour. Technol.* 2006;97:2065-2070.
27. Shen J, Zhu S, Liu X, Zhang H, Tan J. Measurement of heating value of rice husk by using oxygen bomb calorimeter with benzoic acid as combustion adjuvant. *Energy Procedia* 2012;17:208-213.
28. Chakraverty A, Mishra P, Banerjee HD. Investigation of thermal decomposition of rice husk. *Thermochim. Acta* 1985;94: 267-275.
29. Hanna SB, Farag LM. Kinetic studies on thermal degradation of treated and untreated rice husk. *Thermochim. Acta* 1985;87:239-247.
30. James J, Rao MS. Silica from rice husk through thermal decomposition. *Thermochim. Acta* 1986;97:329-336.
31. Vlaev LT, Markovska IG, Lyubchev LA. Non-isothermal kinetics of pyrolysis of rice husk. *Thermochim. Acta* 2003;406:1-7.
32. Biagini E, Fantei A, Tognotti L. Effect of the heating rate on the devolatilization of biomass residues. *Thermochim. Acta* 2008;472:55-63.
33. Shen DK, Gua S, Luo KH, Bridgwater AV, Fang MX. Kinetic study on thermal degradation of woods in an oxidative environment. *Fuel* 2009;88:1024-1030.
34. Chin BLF, Yusup S, Shoaibi AA, Kannan P, Srinivasakannan C, Sulaiman SA. Kinetic studies of co-pyrolysis of rubber seed shell with high-density polyethylene. *Energ. Convers. Manage.* 2014;87:746-753.
35. Sait HH, Hussain A, Salema AA, Ani FN. Pyrolysis and combustion kinetics of date palm biomass using thermogravimetric analysis. *Bioresour. Technol.* 2012;118:382-389.
36. Boxiong S, Qinlei. Study on MSW catalytic combustion by TGA. *Energ. Convers. Manage.* 2006;47:1429-1437.
37. Leroy V, Cancellieri D, Leonib E, Rossib JL. Kinetic study of forest fuels by TGA: Model-free kinetic approach for the prediction of phenomena. *Thermochim. Acta* 2010;497:1-6.
38. Aboyade AO, Hugo TJ, Carrier M, et al. Non-isothermal kinetic analysis of the devolatilization of corn cobs and sugarcane bagasse in an inert atmosphere. *Thermochim. Acta* 2011;517: 81-89.
39. Shen J, Zhu S, Liu X, Zhang H, Tan J. The prediction of elemental composition of biomass based on proximate analysis. *Energ. Convers. Manage.* 2010;51:983-987.
40. Rozainee M, Ngo SP, Salema AA, Tan KG. Computational fluid dynamics modeling of rice husk combustion in a fluidized bed combustor. *Powder Technol.* 2010;203:331-347.
41. Ghani WA, Alias AB, Savory RM, Cliffe KR. Co-combustion of agricultural residues with coal in a fluidized bed combustor. *Waste Manage.* 2009;29:767-773.
42. Kuprianov VI, Janvijitsakul K, Permchart W. Co-firing of sugar cane bagasse with rice husk in a conical fluidized-bed combustor. *Fuel* 2006;85:434-442.
43. Nhuchhen DR. Prediction of carbon, hydrogen, and oxygen composition of raw and terrified biomass using proximate analysis. *Fuel* 2016;180:348-358.
44. Klasson KT. Biochar characterization and a method for estimating biochar quality from proximate analysis results. *Biomass Bioenerg.* 2017;96:50-58.
45. Majumder AK, Jain R, Banerjee P, Brnwal IP. Development of a new proximate analysis based correlation to predict calorific value of coal. *Fuel* 2008;87:3077-3081.
46. Kumar S, Singh RK. Pyrolysis kinetics of waste high-density polyethylene using thermogravimetric analysis. *Int. J. Chem. Tech. Res.* 2014;6:131-137.
47. Adrados A, de Marco I, Caballero BM, López A, Laresgoiti MF, Torres A. Pyrolysis of plastic packaging waste: A comparison of plastic residuals from material recovery facilities with simulated plastic waste. *Waste Manage.* 2012;32:826-832.
48. Chattopadhyay J, Kim C, Kim R, Pak D. Thermogravimetric characteristics and kinetic study of biomass co-pyrolysis with plastic. *Korean J. Chem. Eng.* 2008;25:1047-1053.
49. NPL National Physics Laboratory. Calorific values of solid, liquid and gaseous fuels [Internet]. E.F.G. Herington: NPL National Physics Laboratory; 1995 [cited 12 December 2017]. Available from: http://www.kayelaby.npl.co.uk/chemistry/3_11/3_11_4.html.
50. Tsuchiya Y, Yoshida T. Pelletization of brown coal and rice bran in Indonesia: Characteristics of the mixture pellets including safety during transportation. *Fuel Process. Technol.* 2017;156:68-71.
51. Burgard DA, Bria CRM. Bridge-based sensing of NO_x and SO_2 emissions from ocean-going ships. *Atmos. Environ.* 2016;136:54-60.
52. Sung Y, Lee S, Kim C, et al. Synergistic effect of co-firing woody biomass with coal on NO_x reduction and burnout during air-staged combustion. *Exp. Therm. Fluid Sci.* 2016;71:114-125.
53. Fan W, Li Y, Guo Q, Chen C, Wang Y. Coal-nitrogen release and NO_x evolution in the oxidant-staged combustion of coal. *Energy* 2017;71:417-426.
54. Andrew TT, Montserrat F. Field-portable-XRF reveals the ubiquity of antimony in plastic consumer products. *Sci. Total Environ.* 2017;584:982-989.